CHIN. PHYS. LETT. Vol. 29, No. 5 (2012) 054213

Tomographic Imaging and Three-Dimensional Reconstruction Based on a High-Gain Optical Parametric Amplifier

YANG Jing(杨晶)[1,3], DU Shi-Feng(杜仕峰)[1], ZHANG Jing-Yuan(张景园)[1,2*], CAO Dong(曹栋)[1,3], CUI Da-Fu(崔大复)[1], PENG Qin-Jun(彭钦军)[1], XU Zu-Yan(许祖彦)[1*]

[1]*RCLPT, Key Lab of Functional Crystal and Laser Technology, Technical Institute of Physics and Chemistry, Chinese Academy of Sciences, Beijing 100190*

[2]*Department of Physics, Georgia Southern University, Statesboro, GA 30460, USA*

[3]*Graduate University of the Chinese Academy of Sciences, Beijing 100190*

(Received 17 January 2012)

Tomographic imaging and three-dimensional reconstruction based on a high-gain picosecond optical parametric amplifier (OPA) is demonstrated. More than 40 dB intensity amplification of the image is achieved from the high-gain OPA. The images of various longitudinal positions of the target are extracted by the gated nature of the OPA, then a three-dimensional (3-D) surface topography of the target is reconstructed. The gated and high-gain property of the OPA allows tomographic optical imaging together with 3-D profile reconstruction of the target in turbid media.

PACS: 42.30.Wb, 42.65.Yj DOI: 10.1088/0256-307X/29/5/054213

Optical tomographic imaging plays an important role in biomedical diagnosis, and remote sensing, especially when signal light propagates in the media with strong scattering. Compared with other optical image amplifiers, such as Raman amplifiers,[1] photorefractive,[2] and stimulated Brillouin scattering,[3] optical parametric amplifiers (OPAs) are competitive due to their combination of high gain,[4–6] low noise figure,[7] and frequency tunability. The availability of gated pulses make it possible to extract the ballistic photons of the weak image after passing through the turbid samples, which has been investigated theoretically and experimentally.[8,9] Because the temporal gate is determined by the pulse width of the pump beam, the shorter the pulse width, the higher the resolution and the greater the signal gain will be, i.e. 40 dB image intensity gain and better than 24 μm longitudinal resolution have been demonstrated with the use of femtosecond pulse lasers.[10,11] However, these reported optical parametric image amplifications focused on the extraction of the ballistic photons, while three-dimensional profiles of the target are always neglected.[8–11]

In this Letter, we report tomographic imaging and three-dimensional (3-D) reconstruction using a high-gain picosecond optical parametric amplifier (OPA). Firstly, a 2-D target is used to quantify the gain to the weak images. More than four orders of magnitude has been achieved in terms of the CCD's output gray-scale value. Secondly, since only the signal within the pulse width of the pump beam can be extracted and amplified, images of a 3-D target at various longitudinal positions are obtained by adjusting the temporal overlap between the signal and pump beams. After that, the surface topography of the 3-D target is reconstructed based on the tomographic images. To our knowledge, it is the first time that a gated OPA has been used for tomographic analysis together with 3-D topography reconstruction.

The experimental setup is schematically illustrated in Fig. 1. The horizontally polarized 532 nm is the second harmonic generation (SHG) output of a picosecond 1064 nm Nd:YAG laser (EKSPLA 2143-C, 10 Hz). The 532 nm laser is attenuated continuously from mJ/pulse to less than 1 nJ/pulse by combining a half-wave plate (HWP), a thin film polarizer (TFP) and neutral density filters (NDFs). After being reflected from M1, the 2-D or 3-D target is illuminated. The scattered signal is collected by imaging lenses L1 and L2, and seeded into the BBO crystal, in which the signal is amplified by a 355-nm pump laser. The distance between the target and the imaging lens is set to be 1000 mm. The magnification of the collecting system is 0.21, indicating that the image is 1.7 mm in diameter, which is significantly smaller than the pump beam and allows for uniform amplification. The weak image of the target with total energy of about 100 pJ is formulated on the surface plane 1 (P1) of the BBO crystal, which is cut at $\theta = 29°$, $\phi = 0°$ for type-I phase-matching (o+o→e) with the dimensions of 8 mm(W) × 5 mm(H) × 8 mm(L). The single-shot weak image is amplified by the BBO-OPA and then the enhanced image is relay-passed by L5 and repositioned at plane 2 (P2), where it is recorded by a cooled 14-bit CCD (CoolSNAP HQ2, Photometrics). The 1 mJ pump beam at 355 nm for the OPA is provided by the third harmonics of the same laser. It passes through a 3:1 telescope system (TS) comprised

*To whom correspondence should be addressed. Email: zyxu@mail.ipc.ac.cn; jyzhang30460@yahoo.com

© 2012 Chinese Physical Society and IOP Publishing Ltd

of two lenses, L3 and L4, and the beam size is reduced from the original 9 mm to 3 mm in diameter to match the lateral dimension of the crystal and to reach the pumping intensity of ∼1.7 GW/cm^2. Spatial and temporal overlaps of the signal and pump beams are achieved by beam steering mirrors M8 and M2 and adjusted by the delay line (DL). The signal beam interacts with the pump beam in the BBO crystal and is amplified by the OPA. The residual pump beam is dumped out by M3 and collected by the beam dump (BD), and NDFs are used to further attenuate the amplified image to avoid saturation of the CCD. To eliminate the influence of the idler beam of the OPA at 1064 nm and the residual pump beam at 355 nm, a narrow band-pass filter (BPF) at 532 nm is used. The BBO crystal is used because it guarantees high gain for a weak image from a large nonlinear coefficient and a reasonable damage threshold. The angle α between the incident beam and the signal-receiving axis is as small as 1.5°.

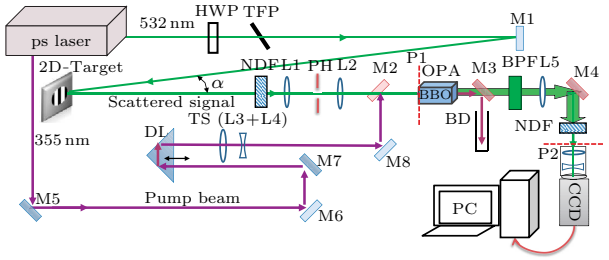


Fig. 1. The experimental setup. See main text for explanations of the abbreviations.

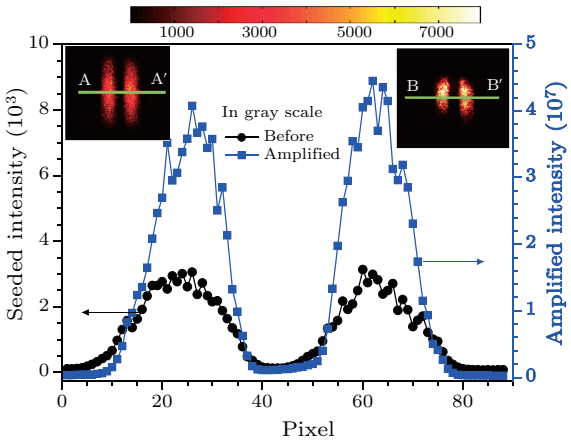


Fig. 2. Image of the 2-D target without amplification (left inset) and amplified images (right inset), and the corresponding intensity profiles along the line $\overline{AA'}$ and $\overline{BB'}$, which are represented by black solid circles and blue solid squares, respectively.

First, the experimental study is carried out by using a Teflon plate as the 2-D target with double 2-mm-wide slots and also separated by 2 mm. The spot size of the beam on the target is 8 mm, which contains two bars in the field of view (FOV), as shown in Fig. 2. At the beginning, the 355 nm pump beam is blocked, and the image is directly recorded by the CCD without using the neutral density filters (NDFs) and the OPA-preamplifier. The HWP is rotated to control the light flux of the signal beam until the real-time image from the PC screen becomes barely detectable by the CCD, as shown by the inset at the upper left corner in Fig. 2. The intensity of the signal measured with the sensitive detector is approximately 100 pJ/pulse.

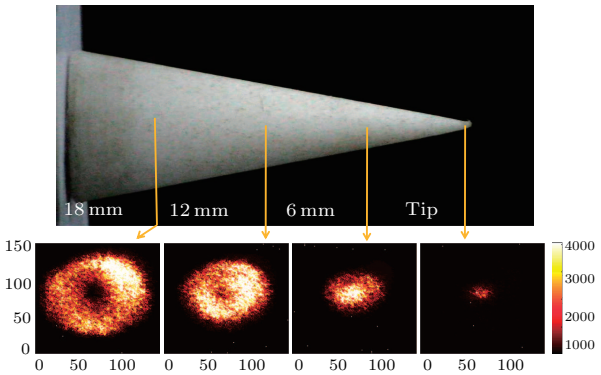


Fig. 3. The opaque Teflon target (upper) and the corresponding tomographic images of the cone (lower) at different positions.

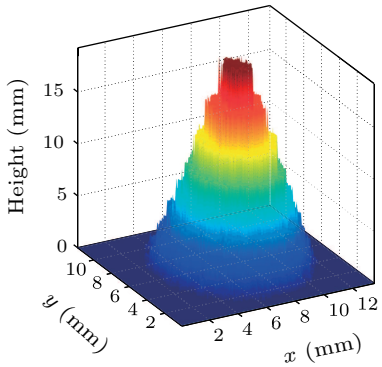


Fig. 4. Surface topography reconstruction of the 3-D cone target based on the tomographic images.

Next, the system is restored as shown in Fig. 1 by putting the NDF back. Evident amplification of the original weak image is observed when the pump beam is introduced. It is much stronger than the previous one even after attenuation by the NDF with an optical density (OD) of 3.8. The image acquired is shown in the inset at the upper-right corner of Fig. 2, the corresponding pump energy is 1 mJ with a 3-mm diameter. The comparison validates the effect of the OPA as an image intensity-amplifier. The vertical size of the amplified image is decreased because of the spatial mismatch between the pump and signal, and this influence can be reduced by phase match optimization and pump intensity distribution homogenization.

To give a quantitative description of the intensity amplification, two horizontal segments $\overline{AA'}$ and $\overline{BB'}$ are used to sample the intensity of the image, and the intensity profile is plotted in Fig. 2. The black

solid circles represent the intensity without the OPA and the blue solid squares represent the intensity after amplification. By taking into account the attenuation of OD = 3.8, which corresponds to a 1.58×10^{-4} transmittance, the averaged peak part of the image has increased from 3×10^3 to more than 4×10^7. Accordingly, an enhancement of more than four orders of magnitude is achieved.

To obtain the tomographic imaging, the optical configuration is nearly the same as Fig. 1, only the 2-D target is replaced with a 3-D target of an opaque Teflon cone as shown in the upper image of Fig. 3. The cone has a 15-mm diameter on the base and 28 mm in length. Its symmetric axis is in the horizontal plane. Because it is collinear with the incident laser beam and angle α is small, the reflected signal contains information about the cone from top to bottom. The time delay line (DL) is used to sample the images of the 3-D target at different longitudinal positions. The HWP is rotated until the background of the original image of the cone is completely eliminated from the CCD. The back-scattered photons of specific time slices, which constitute the images of the corresponding longitudinal location, are selected by the gate pulse of the pulse beam, which is adjustable. By considering the roundtrip, the 20 ps pulse width of the pumping laser is longitudinally equivalent to a 3 mm span, which is very short compared with the 20-mm long target thus enabling well-resolved surface tomographic imaging. An increment of 1 mm is chosen in the translational scan so that the resolution of the scan ensures continuous recording of images within the total 20-mm scan range. Moreover, the imaging lens needs to be optimized to make the depth of field longer than the scan range. It is a precondition that the captured images during the scan all are well-resolved. Four of the recorded images are picked out, as shown on the lower part of Fig. 3. They are the tomographic images at the tip, and then 6 mm, 12 mm, 18 mm from the tip, respectively.

By increasing the temporal delay, the tomographic slice moves from the tip to the bottom of the cone, which can be easily recognized from the increasing radius of its external profile, as shown in the lower part of Fig. 3. When the series of images are obtained, the grayscale images are read by the computers and converted into matrixes. By combining these matrixes and the longitudinal position of each layer, the 3-D profile of the target is reconstructed by using a home-developed computer program. The result is shown in Fig. 4, and it can be seen that it coincides well with the target.

Technically, a non-collinear scheme which can minimize the influence of superfluorescence under weak signal, and atto-Joule or even lower detection sensitivity can be achieved with both femtosecond and picosecond OPAs.[5,6] These results indicate that the input intensity of the image could be further reduced when the OPA configuration is updated. At the same time, further improvements are also considered such as using crystals with a larger acceptance angle under phase match condition so that a better spatial resolution can be achieved, and using a pump intensity distribution homogenizer.[9] The inherent high-gain and temporal gated property of the OPA makes optical tomography possible in the diffused media since embedded plane target imaging has been successfully demonstrated.[11]

In summary, tomographic imaging and 3-D reconstruction based on a high-gain picosecond OPA is demonstrated. For the 2-D gated imaging, amplification with more than four orders of magnitude is obtained. By extracting tomographic signals from the different time slices, the surface topography of a 3-D target can be reconstructed. Hopefully, with its gated and high-gain property, an optical parametric amplifier could be used in ranging gated imaging such as tomography and remote sensing with high longitudinal resolution. When the wavelength is tuned to the low loss window, non-invasive tomographic imaging in the turbid media can be obtained.

References

[1] Moon J A, Mahon R, Duncan M D and Reintjes J 1994 *Opt. Lett.* **19** 1234
[2] Vainos N A and Gower M C 1991 *Opt. Lett.* **16** 363
[3] Sternklar S, Jackel S, Chomsky D and Zigler A 1990 *Opt. Lett.* **15** 616
[4] Du S F, Zhang D X, Shi Y X, Wang S, Li Q, Feng B H and Zhang J Y 2008 *Opt. Commun.* **281** 2638
[5] Han X F, Chen X H, Weng Y X and Zhang J Y 2007 *J. Opt. Soc. Am.* B **24** 1633
[6] Du S F, Zhang D X, Shi Y X, Wang S, Li Q, Feng B H and Zhang J Y 2008 *Opt. Commun.* **281** 5014
[7] Choi S K, Vasilyev M and Kumar P 1999 *Phys. Rev. Lett.* **83** 1938
[8] Tolguenec G L Lantz E and Devaux F 1997 *Appl. Opt.* **36** 8292
[9] Devaux F and Lantz E 1995 *Opt. Commun.* **114** 295
[10] Watson J, Georges P, Lepine T, Alonzi B and Brun A 1995 *Opt. Lett.* **20** 231
[11] Doule C, Lepine T, Georges P and Brun A 2000 *Opt. Lett.* **25** 353